Chemical Science

ROYAL SOCIETY OF CHEMISTRY

EDGE ARTICLE

View Article Online
View Journal | View Issue

Cite this: *Chem. Sci.*, 2021, **12**, 15399

All publication charges for this article have been paid for by the Royal Society of Chemistry

Construction of sterically congested oxindole derivatives *via* visible-light-induced radical-coupling†

Yanling Shen, Ning Lei, Cong Lu, Dailin Xi, Xinxin Geng, Pan Tao, Zhishan Su and Ke Zheng *

Received 23rd September 2021
Accepted 3rd November 2021

DOI: 10.1039/d1sc05273j

rsc.li/chemical-science

The oxindole scaffold represents an important structural feature in many natural products and pharmaceutically relevant molecules. Herein, we report a visible-light-induced modular methodology for the synthesis of complex 3,3′-disubstituted oxindole derivatives. A library of valuable fluoroalkyl-containing highly sterically congested oxindole derivatives can be synthesized by a catalytic three-component radical coupling reaction under mild conditions (metal & photocatalyst free, >80 examples). This strategy shows high functional group tolerance and broad substrate compatibility (including a wide variety of terminal or non-terminal alkenes, conjugated dienes and enynes, and a broad array of polyfluoroalkyl iodide and oxindoles), which enables modular modification of complex drug-like compounds in one chemical step. The success of solar-driven transformation, large-scale synthesis, and the late-stage functionalization of bioactive molecules, as well as promising tumor-suppressing biological activities, highlights the potential for practical applications of this strategy. Mechanistic investigations, including a series of control experiments, UV-vis spectroscopy and DFT calculations, suggest that the reaction underwent a sequential two-step radical-coupling process and the photosensitive perfluoroalkyl benzyl iodides are key intermediates in the transformation.

Introduction

The oxindole scaffold is one of the most abundant structural units in a wide variety of natural products, agrochemicals, and pharmaceutical agents.[1] In particular, 3,3′-disubstituted oxindoles with one or more all-carbon quaternary centers play a significant role in a number of biologically active[2] and medicinal agents[3] (scheme 1A), benefitting from numerous distinct properties arising from their fully substituted carbon centers. Therefore, extensive efforts are focused on developing an efficient strategy for the construction of these compounds.[4] One classical method for accessing this class of compounds is nucleophilic substitution of 3-substituted oxindoles, taking advantage of their high nucleophilicity at the C3-position of oxindoles, and most of these methods can be rendered enantioselective through the action of asymmetric catalysts (Scheme 1B, left part).[4c–g] However, the practical utilization of these methods is largely limited to the unhindered substrates (primary or secondary), and the extension to tertiary substrates is still a challenge due to their increased steric hindrance, as well as the limitations of commercially available tertiary substrates.[5] Despite extensive efforts made in substitution reactions, a small number of radical–radical coupling processes have been reported as an alternative protocol for the synthesis of 3,3′-disubstituted oxindoles. However, these strategies have major limitations in complex molecular settings (Scheme 1B, right part).[6] Considering the increasing demand of drug discovery for flexible modulation of 3,3′-disubstituted oxindole derivatives with structural complexity, the discovery of new protocols to access these important frameworks from ubiquitous starting materials is highly desired.

Fluorine-containing groups in organic molecules serve as versatile and valuable motifs in the agrochemical industry, medicinal chemistry and materials science, and have the potential to exert profound changes in the lipophilicity, solubility, metabolic stability, and bioavailability properties of molecules in drug discovery.[7] The iodoperfluoroalkylation of olefins is an efficient transformation for accessing this class of compounds relying on the use of photochemistry, in which the commercially available perfluoroalkyl halides (R_f–X) were used as powerful and versatile precursors to generate electrophilic perfluoroalkyl radicals.[8] Numerous elegant reports of photocatalytic iodoperfluoroalkylation of alkenes using organic bases or photocatalysts have been well established.[9] However, for

Key Laboratory of Green Chemistry & Technology, Ministry of Education, College of Chemistry, Sichuan University, Chengdu 610064, P. R. China. E-mail: kzheng@scu.edu.cn

† Electronic supplementary information (ESI) available: Detailed experimental procedures, computational details, and spectroscopic data for all new compounds. CCDC 2090721, 2096415 and 2096414. For ESI and crystallographic data in CIF or other electronic format see DOI: 10.1039/d1sc05273j

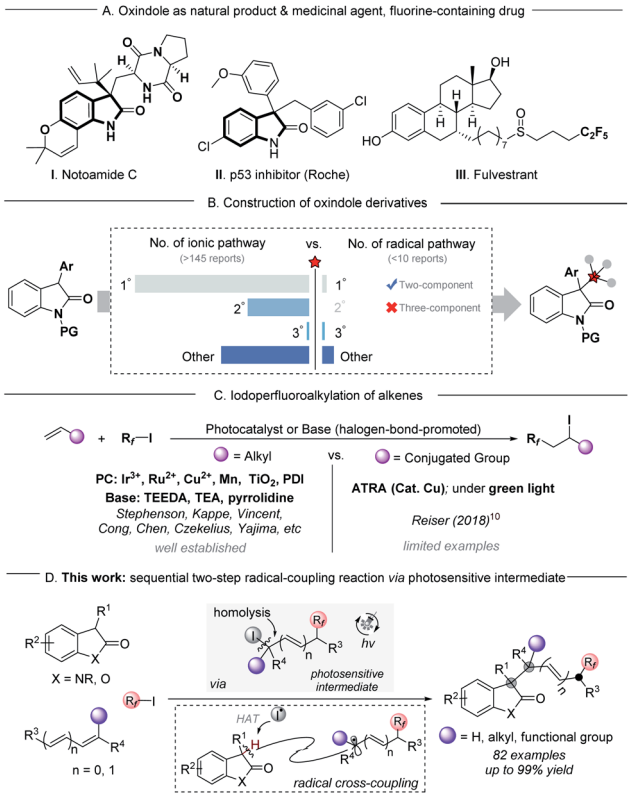

Scheme 1 Sequential two-step radical-coupling reaction *via* photosensitive intermediates.

most of them, the radical acceptors were limited to alkyl alkenes, and only a limited number of analogous transformations have been reported for conjugated alkenes (Scheme 1C).[10] This was likely to originate from the instability of conjugated carbon radical intermediates,[11,12] or iodoperfluoroalkylation products such as sensitive benzyl iodides, especially the tertiary benzyl iodides with steric hindrance.[10a,13] We questioned whether or not such unstable, photosensitive benzyl iodides could be used as intermediates for the next transformations by secondary excitation under irradiation. If it works, it should be possible to design a sequential multistep radical-coupling process to construct functionally and structurally diverse products from ubiquitous starting materials under mild conditions.

Continuing our interest in developing new photochemical methods,[14] we present herein visible-light-driven highly selective three-component radical coupling reactions for the construction of fluoroalkyl-containing highly sterically congested oxindole derivatives in a single step, which would require multistep syntheses using other methods (>80 examples, Scheme 1D). This transformation could successfully be applied to a wide variety of conjugated alkenes, including terminal or non-terminal styrene derivatives, dienes and enynes. The potential efficacy of this new approach was evidenced by the success of gram-level synthesis, late-stage functionalization, and modular modification of known bioactive pharmaceuticals.

Table 1 Reaction optimization[a]

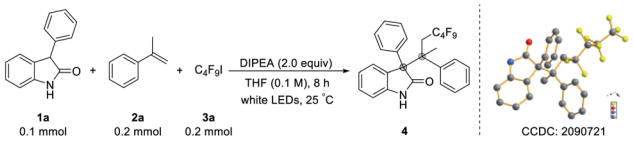

Entry	Variation from standard conditions	Yield[b]%
1	None	88
2	395 nm LED	75
3	525 nm LED	Trace
4	DMF as solvent	69
5	CH_3OH as solvent	66
6	Cs_2CO_3 instead of DIPEA	43
7	K_2CO_3 instead of DIPEA	73
8	Aniline instead of DIPEA	Trace
9	0.2 M or 0.05 M	77
10	Heat to 40 °C	88[c]
11	Without DIPEA	Trace
12	In air or without light	Trace

[a] Reaction conditions: **1a** (0.1 mmol), **2a** (0.2 mmol), **3a** (0.2 mmol) and DIPEA (0.2 mmol) in THF (1.0 mL) were irradiated with 10 W white LEDs under N_2 at 25 °C. [b] Yield of the isolated product; *dr* (diastereomeric ratio) of product was 1 : 1. [c] Reaction time: 4 h. DIPEA = *N*,*N*-diisopropylethylamine.

Results and discussion

On the basis of our hypothesis, we first selected 3-phenylindolin-2-one (**1a**), α-methyl-styrene (**2a**) and perfluorobutyl iodide (**3a**) as model substrates for optimization studies. After exploring different reaction conditions, the best results were accomplished with DIPEA as the base additive under white light irradiation in THF under N_2, affording three-component coupling product **4** in 88% isolated yield with a 1 : 1 *dr* value (Table 1, entry 1). Among the light sources screened, white light proved to be the most effective at facilitating transformation and green light could not promote the reaction (Table 1, entries 2–3 and Table S1†). Several other common organic solvents led to slightly lower yields (Table 1, entries 4–5 and Table S2†). When using inorganic base Cs_2CO_3 or K_2CO_3 instead of DIPEA, lower yields were observed, and aniline completely shut down the reaction (Table 1, entries 6–8). Either higher or lower concentrations of the reaction mixture gave decreased yields (Table 1, entry 9). To our delight, the reaction time could be significantly shortened with a similar outcome at higher temperature (Table 1, entry 10). A series of control experiments indicated that the base additive DIPEA, light, and N_2 atmosphere were all crucial for this reaction (Table 1, entries 11–12).

With the optimized reaction conditions in hand, we first explored the scope of 3-substituted oxindoles (Table 2). Remarkably, the reaction proved suitable for the synthesis of highly sterically congested quaternary centers even in good to excellent yields (**5–29**). The reactions performed well with a variety of 3-aryl substituted oxindoles with electron-neutral, electron-donating, and electron-withdrawing substituents, giving the corresponding products in excellent yields (**5–16**).

Table 2 Scope of the oxindole derivatives[a]

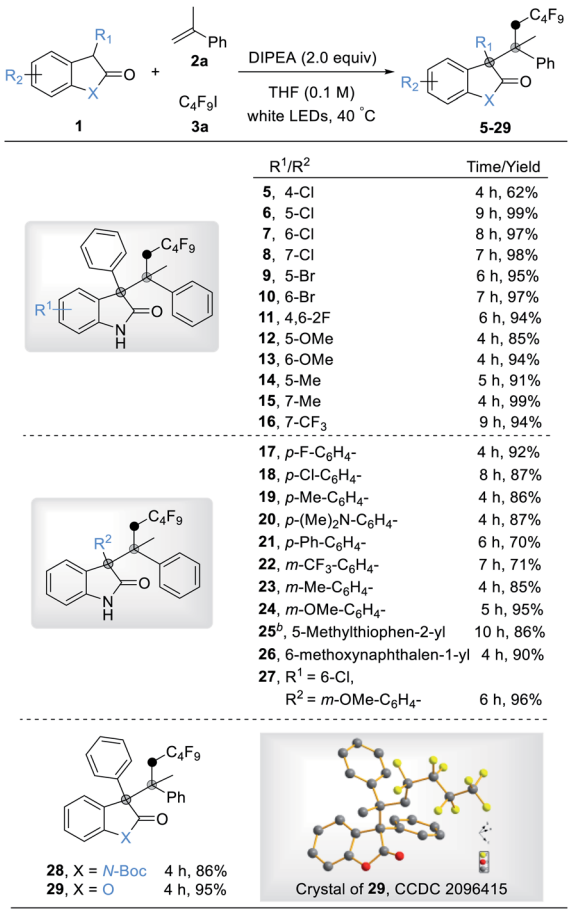

[a] Reaction conditions: **1** (0.1 mmol), **2a** (0.2 mmol), **3a** (0.2 mmol), and DIPEA (0.2 mmol) in THF (1.0 mL) were irradiated with 10 W white LEDs under N_2 at 40 °C. Yield of the isolated product. The *dr* (diastereomeric ratio) of the product was 1 : 1 unless otherwise noted. [b] *dr* = 1 : 2.

The oxindole with 4-substituents on the aromatic ring produced the products with slightly lower yield (**5**) due to its steric crowding adjacent to the reactive site. Substituents on the aromatic ring of the 3-aryl oxindole with a variety of functional groups afforded the product in good to excellent yields (**17–25**). To our delight, 3-heterocyclic- and 3-naphthyl- substituted oxindoles were also well tolerated under optimized conditions (**26** and **27**). The substituted group on the nitrogen of oxindoles does not affect the outcome (86%, **28**), and benzofuranone gave the desired product in high yield (95%, **29**).

Having established a broad scope for oxindoles, our attention was turned to the scope with respect to alkenes. As shown in Table 3, both simple and functionalized alkenes were good coupling partners under these conditions (**30–66**). Substituted styrenes with electron-donating and electron-withdrawing groups gave the corresponding products in good yields (**30–36**). Even more electron-deficient pentafluoro-substituted styrene (**37**) could be used effectively, producing the desired product in moderate yield. 2-Vinylnaphthalene and 9-vinylanthracene underwent the reaction smoothly to give the corresponding products in high yields (**38** and **39**). The boronic acid (**40**) and carboxyl group (**41**) were well tolerated, thus making this protocol suitable for synthesis of oxindole derivatives without protective groups. Disubstituted alkenes were also well-tolerable with excellent yields (**42–43**). Additionally, the product 43 gave a higher *dr* value (10 : 1) due to its steric hindrance. Heterocyclic olefins gave the products in moderate yields due to the lability of the heterocyclic system (**44–45**). Notably, the reaction could accommodate thiophene ethylene, and a mixture of 1,2-addition and 1,6-addition products was observed in acceptable yield (**46**). To our delight, a wide range of highly functionalized 1,1-disubstituted alkenes such as α-bromo (**47**), α-boronic ester (**48**), α-trifluoromethyl (**49**), and α-carboxyl (**50**) could be successfully used in this radical-based process to give three-component coupling products in synthetically useful yields, and an excellent *dr* was obtained for product **50** (*dr* > 20 : 1), opening avenues for further synthetic operations. Meanwhile, a highly selective reaction occurred at the aryl alkene position of the substrate, which contained both an aryl alkene and an alkyl alkene moiety, to obtain an exclusive product in excellent yield (**51**). Non-terminal styrenes such as 1,2-dihydronaphthalene (**52**), 1-cyclobuten-1-ylbenzene (**53**), and 1*H*-indene (**54**) also performed well to give congested products in moderate yields.

It was worth noting that conjugate olefins such as 1,3-dienes (**55–57**) proved to be competent partners in the reaction, highlighting the extraordinary substrate scope of this strategy. When 1,3-butadiene and cyclohexa-1,3-diene were subjected to this protocol, a mixture of 1,2-addition and 1,4-addition products was obtained in high yields (**55** and **56**), while only 1,4-addition product **57** was obtained for 2,3-dimethylbuta-1,3-diene. Notably, 1,3-enynes could also be used as radical acceptors to form substituted allenyl (1,4-adducts) or alkynyl (1,2-adducts) derivatives under the optimized conditions, which are important structural motifs found in pharmaceuticals and considered as key intermediates in the synthesis of complex molecules. Compared to the product mixture obtained with 2-methyl substituted enynes (**58** and **59**), 2-phenyl substituted enynes gave the 1,4-addition product allenes (**60** and **61**) in excellent yields exclusively. The excellent functional group compatibility and broad substrate scope of this strategy encouraged us to evaluate its application in the late-stage functionalization of bioactive molecules. Several drugs and natural product derivatives such as isoeugenol, estrone, menthol, flavanone and galactose were subjected to the optimized reaction conditions, resulting in the desired complex products in good to excellent yields (**62–66**).

To illustrate the utility of this new transformation with respect to drug discovery, we applied this radical three-component coupling reaction to modify p53 inhibitor II (Roche). Using a variety of polyfluoroalkyl halides as the fluorinating reagent, a series of polyfluorinated analogues (**67–78**) of inhibitor II were furnished in high yields under mild conditions (Table 4). The estrogen derivatives were also tolerable in our system to deliver corresponding products in good yields after a two-step reaction (**79–82**). The success of sunlight-driven

Table 3 Scope of the alkenes, dienes and enynes[a]

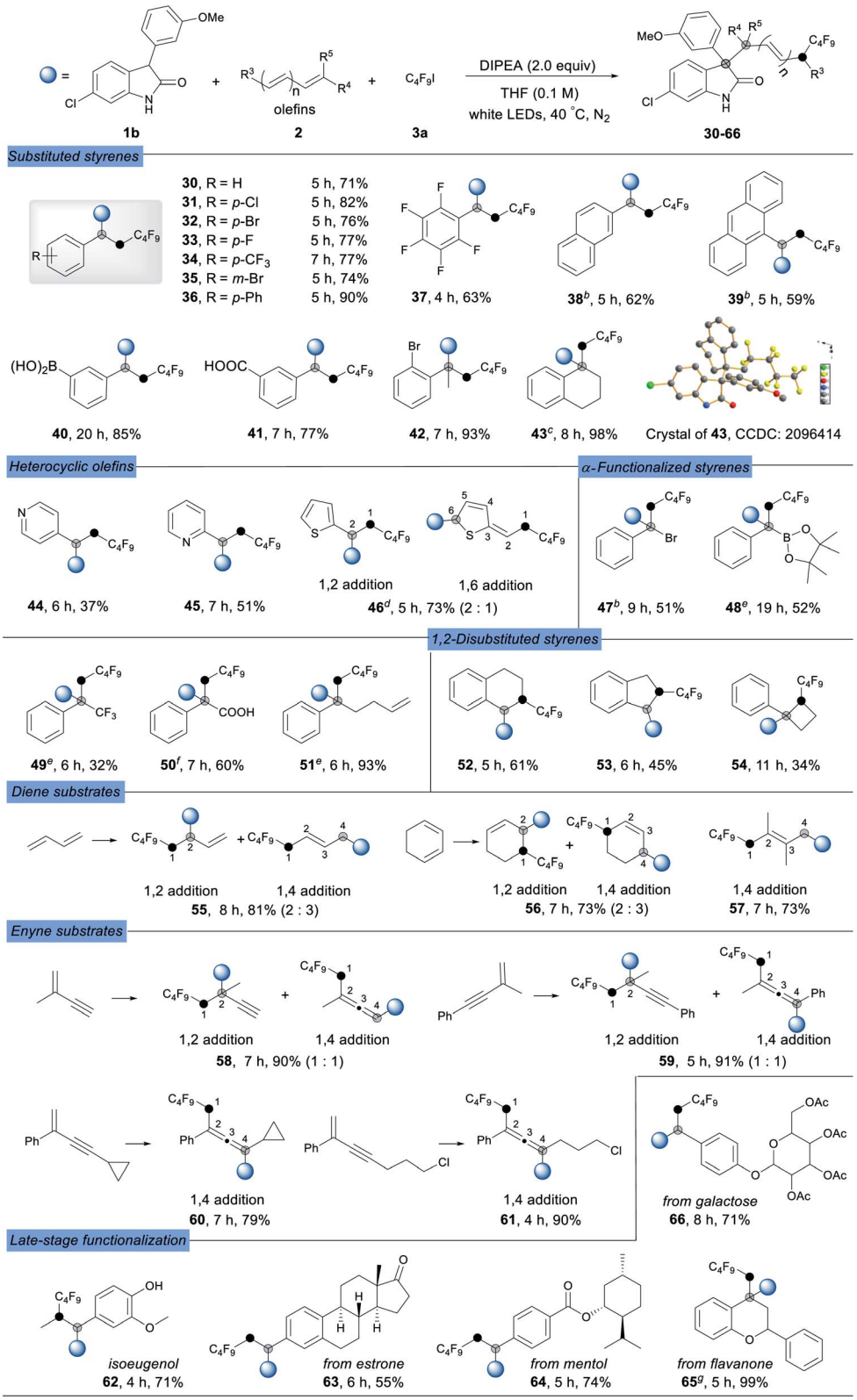

[a] Reaction conditions: **1** (0.1 mmol), **2a** (0.2 mmol), **3a** (0.2 mmol), and DIPEA (0.2 mmol) in THF (1.0 mL) were irradiated with 10 W white LEDs under N_2 at 40 °C. Yield of the isolated product. The *dr* (diastereomeric ratio) of the product was 1 : 1 unless otherwise noted. [b] *dr* = 2 : 3. [c] *dr* = 10 : 1. [d] Detected by ^{1}H NMR, *Z* : *E* = 2 : 1 (1,6 addition). [e] *dr* = 4 : 1. [f] *dr* > 20 : 1. [g] *dr* = 5 : 2 : 3.

Table 4 Preparation of pharmaceutical analogues[a]

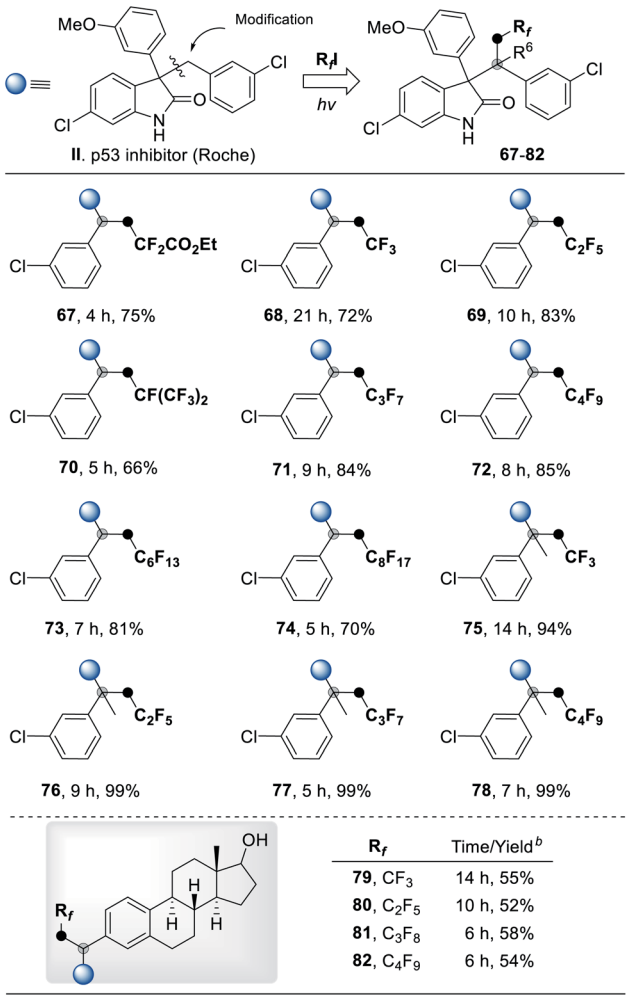

R_f	Time/Yield[b]
79, CF_3	14 h, 55%
80, C_2F_5	10 h, 52%
81, C_3F_8	6 h, 58%
82, C_4F_9	6 h, 54%

[a] Reaction conditions: **1b** (0.1 mmol), **2** (0.2 mmol), **3a** (0.2 mmol), and DIPEA (0.2 mmol) in THF (1.0 mL) were irradiated with 10 W white LEDs under N_2 at 40 °C. Yield of the isolated product. The *dr* (diastereomeric ratio) of the product was 1 : 1. [b] Two steps, see the ESI† for exact experimental procedures.

transformation (**78**, 84% yield) and gram-scale synthesis (**78**, 1.05 g, 65% yield) revealed the potential of this strategy in industrial applications (for more details see ESI, Fig. S6†). To demonstrate the biological application of these analogues, some of the polyfluorinated oxindole derivatives were assayed for growth inhibitory activities on the human cancer cell line MCF-7 (breast cancer); compared to p53 inhibitor II, the antitumor activity of fluorine-modified compounds was significantly improved (Table 5 and S5†). Further SAR of these new scaffolds is currently in progress in our groups.

Table 5 *In vitro* antitumor activity of selected fluoroalkyl-containing oxindole derivatives (IC_{50}, μM)

Compounds	p53 inhibitor II		**32**	**56**	**68**
IC_{50} (MCF-7)	38.95		21.16	21.99	16.73
Compounds	**69**	**70**	**71**	**72**	**76**
IC_{50} (MCF-7)	22.63	7.23	20.60	21.04	20.99

Having established a broad scope for the synthesis of polyfluorinated oxindole derivatives, our attention was focused on the mechanism of this three-component radical-coupling reaction. UV-vis spectroscopic measurements on various combinations of **1b**, **2b**, and **3a** with different bases were first performed. Compared to the marked yellow color and red-shift of the UV-vis absorption observed by using strong bases such as Cs_2CO_3 or DUB as additives (the $R_f^{\cdot}$ was initiated by the photoconductive EDA complex of enolate with C_4F_9I, see Fig. S7 and S8†), no color change and no detectable red-shift with a mixture of DIPEA, **1b** and C_4F_9I were observed. These results indicated that the possibility of the EDA complex of substrates with DIPEA as the base additive was excluded (for more control experiments see ESI, Tables S6 and S7†). Moreover, the iodoperfluoroalkylation product **85** was obtained during the reaction course, even without oxindole under the standard conditions (Scheme 2a). We monitored this process by ^1H NMR and found that benzyl iodide **85** was unstable and would rapidly decompose under white light irradiation (see ESI, Fig. S9†). This outcome was different from Reiser's work, in which the iodoperfluoroalkylation product **85** can be obtained in high yield due to its stability under green light.[10] Meanwhile, the results of light on/off experiments suggested that the formation of **85** did not occur by the chain process (see ESI, Fig. S9†), which was consistent with the previous reports.[10a,15] We considered that in our process, this unstable, photosensitive benzyl iodide **85** might be the key intermediate for the next coupling step.

To gather direct experimental evidence, the intermediate **85** was synthesized and subjected to the optimized reaction conditions. To our delight, compound **85** showed a noticeable reactivity toward **1b** and product **30** was obtained in good yield with 10% dimerization product **83** of oxindole. In the absence of

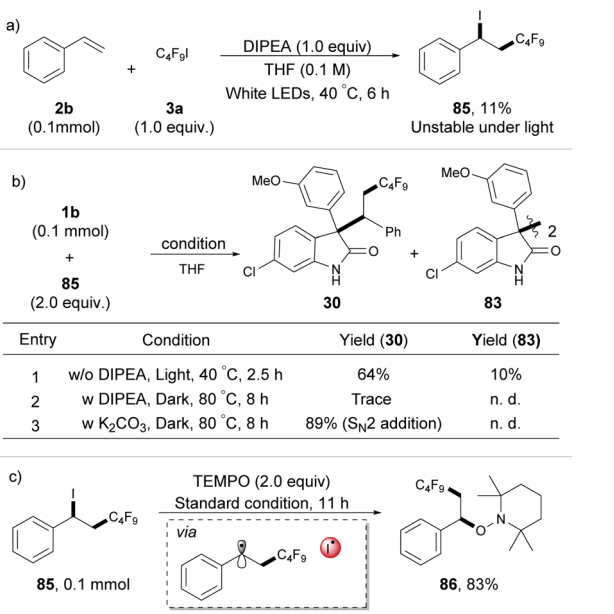

Scheme 2 Control experiments.

light, compared to the high yield obtained with K_2CO_3 (S_N2 addition), only a trace amount of the desired product **30** was detected in the presence of DIPEA at 80 °C in the dark for 8 h (Scheme 2b),[16] indicating that **1b** and **85** were more likely to undergo a radical coupling process than a nucleophilic process under standard conditions. Additionally, the benzyl radical captured product **86** was obtained in 83% yield (Scheme 2c) when the radical scavenger TEMPO and **85** were irradiated directly in THF. These results provided a piece of direct evidence for the formation of the benzyl radical and I˙ radical as key intermediates by homolysis of the C–I bond of photosensitive benzyl iodide **85** under irradiation during the transformation, as well as the reaction undergoing a radical-coupling pathway. These can also explain why a low yield was observed for the iodoperfluoroalkylation product **85** in Scheme 2a (due to the photolysis of **85** under light irradiation).

After demonstrating that iodoperfluoroalkylation product **85** was a key intermediate during the transformation, subsequent efforts were aimed at confirming the essential HAT substance that formed the oxindole radical in the HAT process (Scheme 3a and b). The two possible HAT reagents for abstracting the hydrogen atom from the oxindole as described here were DIPEA$^{\cdot+}$ (from photoexcitation of the XB adduct of DIPEA and C_4F_9I) and I˙ (from homolysis of photosensitive intermediate **85**). As shown in Scheme 3a, no dimerization product **83** was observed when the mixture of oxindole **1b** and C_4F_9I was subjected to the optimized reaction conditions, indicating that DIPEA$^{\cdot+}$ was not a HAT reagent in our strategy. This was further supported by the DFT calculation of radical I˙ with a lower energy barrier in the HAT process (6.6 kcal mol^{-1} for I˙ *vs.* 33.9 kcal mol^{-1} for DIPEA$^{\cdot+}$). The radical clock experiment of α-cyclopropylstyrene **2d** gave the ring-opening product **87** in 87% yield with no dimerization product **83**, suggesting that no radical I˙ was produced in the transformation because the product **87** was stable under light irradiation (Scheme 3b). This was further supported by DFT calculations.[17] Together with DFT calculations and control experiments, we considered that the I˙ radical was the HAT reagent in this process, which was generated from the photolysis of photosensitive intermediate **85**.

Based on the above mechanistic results and previous reports, the proposed mechanism for the radical three-component coupling reaction is depicted in Scheme 3. Upon visible-light irradiation, the XB (halogen bond) complex of DIPEA and perfluoroalkyl iodide **3** is excited and generates the fluoroalkyl

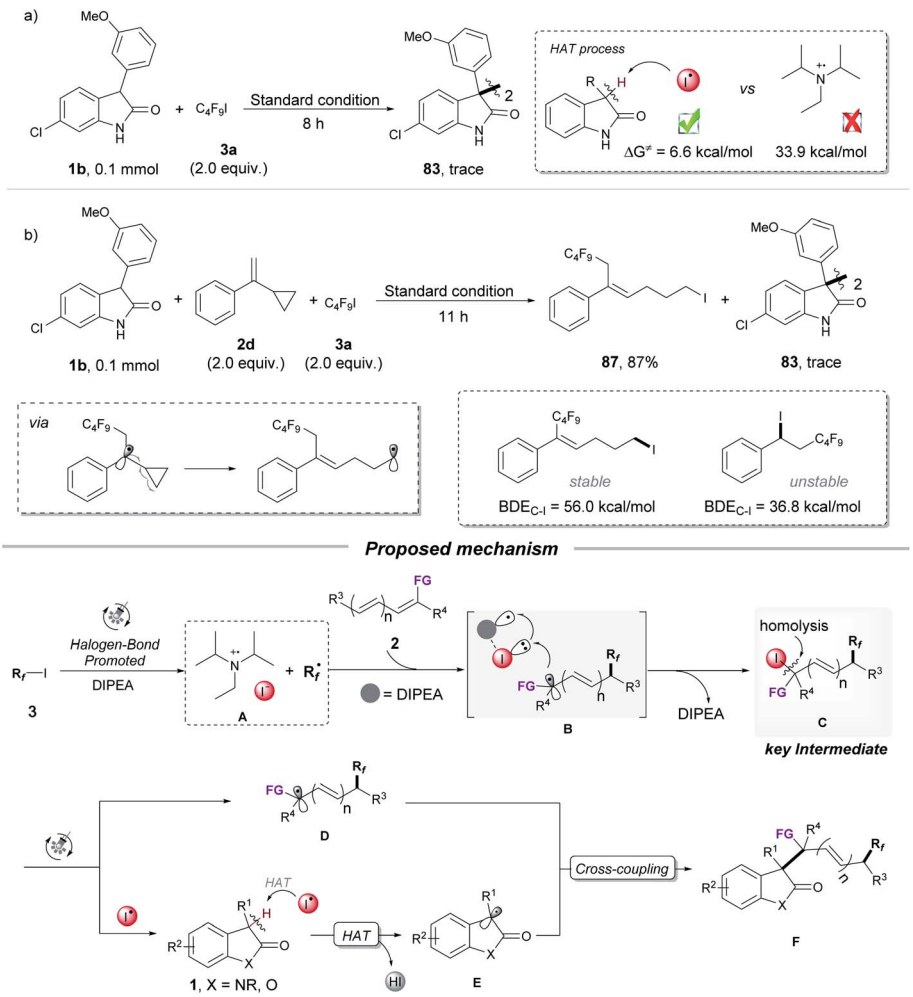

Scheme 3 Control experiments and proposed mechanism.

radical $R_f^{\bullet}$ and complex **A** (DIPEA$^{\bullet+}$---I$^-$).[9f,i,18] The fluoroalkyl radical $R_f^{\bullet}$ adds to the olefin **2** to form a new radical, which reacts with complex **A**, leading to the key photosensitive intermediate **C** (iodoperfluoroalkylation product). The iodine radical I$^{\bullet}$ and radical **D** are generated by photolysis of intermediate **C** under light irradiation. The resulting radical I$^{\bullet}$ acts as a HAT reagent, abstracting the hydrogen atom from oxindole **1** to generate the persistent oxindole radical **E**. Finally, the combination of the radical **D** with the oxindole radical **E** affords the three-component coupling product **F**.

Conclusions

In summary, we have reported a photocatalytic three-component radical coupling reaction for the modular assembly of fluoroalkyl-containing oxindole derivatives. This procedure employs readily accessible or commercially available materials to deliver a series of functional and structural oxindoles with adjacent all-carbon quaternary centers in one chemical step, which are difficult to access by other methods. A wide variety of alkenes including terminal or non-terminal alkenes and conjugated dienes and enynes are successfully applied to this strategy. Moreover, we demonstrate the utility of this strategy in rapid and scalable synthesis of the known pharmaceutical analogues. Detailed mechanistic studies disclose that the photosensitive fluorobenzyl iodides are the key intermediates for this sequential multistep radical-coupling reaction. We anticipate that this simple and mild approach will likely be of interest to chemists both in academic and industrial fields. Further explorations of the biological activity of these new fluorine-modified oxindole compounds are underway in our laboratory.

Data availability

All experimental and computational data in this manuscript are available in the ESI.† Crystallographic data for compound **4**, **29** and **43** have been deposited at the CCDC 2090721, 2096415 and 2096414, respectively.

Author contributions

K. Z. and Y. L. S. conceived the idea for this work and designed the experiments. Y. L. S., C. L., and N. L. performed and analyzed the experiments. Z. S. S. and Y. L. S. performed the theoretical study. P. T., D. L. X., and X. X. G. synthesized some of the substrates. K. Z. supervised the entire project. All authors discussed the results and helped in writing the manuscript.

Conflicts of interest

There are no conflicts to declare.

Acknowledgements

We thank the Xiaoming Feng laboratory (SCU) for access to equipment and Yuqiao Zhou for X-ray structural analysis. We also thank the comprehensive training platform of the Specialized Laboratory in the College of Chemistry at Sichuan University for compound testing. Funding: we acknowledge support from the National Natural Science Foundation of China (Nos. 21602142), Sichuan Science and Technology Program (Nos. 2020YJ0301), and the Fundamental Research Funds for the Central Universities.

Notes and references

1 (*a*) N. H. Greig, X. F. Pei, T. T. Soncrant, D. K. Ingram and A. Brossi, *Med. Res. Rev.*, 1995, **15**, 3–31; (*b*) J. Song, D.-F. Chen and L.-Z. Gong, *Natl. Sci. Rev.*, 2017, **4**, 381–396; (*c*) A. J. Boddy and J. A. Bull, *Org. Chem. Front.*, 2021, **8**, 1026–1084.

2 H. Kato, T. Yoshida, T. Tokue, Y. Nojiri, H. Hirota, T. Ohta, R. M. Williams and S. Tsukamoto, *Angew. Chem., Int. Ed.*, 2007, **46**, 2254–2256.

3 (*a*) C. Hulme, G. B. Poli, F.-C. Huang, J. E. Souness and S. W. Djuric, *Bioorg. Med. Chem. Lett.*, 1998, **8**, 175–178; (*b*) M. K. Christensen, K. D. Erichsen, C. Trojel-Hansen, J. Tjornelund, S. J. Nielsen, K. Frydenvang, T. N. Johansen, B. Nielsen, M. Sehested, P. B. Jensen, M. Ikaunieks, A. Zaichenko, E. Loza, I. Kalvinsh and F. Bjorkling, *J. Med. Chem.*, 2010, **53**, 7140–7145.

4 (*a*) Y. Ping, Y. Li, J. Zhu and W. Kong, *Angew. Chem., Int. Ed.*, 2019, **58**, 1562–1573; (*b*) A. D. Marchese, E. M. Larin, B. Mirabi and M. Lautens, *Acc. Chem. Res.*, 2020, **53**, 1605–1619; (*c*) F. Zhou, Y.-L. Liu and J. Zhou, *Adv. Synth. Catal.*, 2010, **352**, 1381–1407; (*d*) R. Dalpozzo, G. Bartoli and G. Bencivenni, *Chem. Soc. Rev.*, 2012, **41**, 7247–7290; (*e*) K. Shen, X. Liu, L. Lin and X. Feng, *Chem. Sci.*, 2012, **3**, 327–334; (*f*) R. Dalpozzo, *Adv. Synth. Catal.*, 2017, **359**, 1772–1810; (*g*) Z. Y. Cao, F. Zhou and J. Zhou, *Acc. Chem. Res.*, 2018, **51**, 1443–1454.

5 (*a*) C. D. Grant and M. J. Krische, *Org. Lett.*, 2009, **11**, 4485–4487; (*b*) B. M. Trost, W. H. Chan and S. Malhotra, *Chem.–Eur. J.*, 2017, **23**, 4405–4414.

6 (*a*) H. Y. Huang, R. Wu, F. Wei, D. Wang and L. Liu, *Org. Lett.*, 2015, **17**, 3702–3705; (*b*) T. Bleith, Q. H. Deng, H. Wadepohl and L. H. Gade, *Angew. Chem., Int. Ed.*, 2016, **55**, 7852–7856; (*c*) H. Y. Huang, L. Cheng, J. J. Liu, D. Wang, L. Liu and C. J. Li, *J. Org. Chem.*, 2017, **82**, 2656–2663; (*d*) J. J. Liu, H. Y. Huang, L. Cheng, Q. Liu, D. Wang and L. Liu, *Org. Biomol. Chem.*, 2018, **16**, 899–903; (*e*) K. Liang, N. Li, Y. Zhang, T. Li and C. Xia, *Chem. Sci.*, 2019, **10**, 3049–3053; (*f*) R. Ohnishi, M. Sugawara, M. Akakabe, T. Ezawa, H. Koshino, Y. Sohtome and M. Sodeoka, *Asian J. Org. Chem.*, 2019, **8**, 1017–1023; (*g*) H. Wu, C. Qiu, Z. Zhang, B. Zhang, S. Zhang, Y. Xu, H. Zhou, C. Su and K. P. Loh, *Adv. Synth. Catal.*, 2019, **362**, 789–794; (*h*) G. Hong, P. D. Nahide and M. C. Kozlowski, *Org. Lett.*, 2020, **22**, 1563–1568; (*i*) M. Sugawara, R. Ohnishi, T. Ezawa, M. Akakabe, M. Sawamura, D. Hojo, D. Hashizume, Y. Sohtome and M. Sodeoka, *ACS Catal.*, 2020, **10**, 12770–12782; (*j*) Y. Sohtome, K. Kanomata and M. Sodeoka, *Bull. Chem. Soc. Jpn.*, 2021, **94**, 1066–1079.

7 (*a*) K. Müller, C. Faeh and F. Diederich, *Science*, 2007, **317**, 1881–1886; (*b*) B. M. Johnson, Y. Z. Shu, X. Zhuo and N. A. Meanwell, *J. Med. Chem.*, 2020, **63**, 6315–6386; (*c*) R. Britton, V. Gouverneur, J.-H. Lin, M. Meanwell, C. Ni, G. Pupo, J.-C. Xiao and J. Hu, *Nat. Rev. Methods Primers*, 2021, **1**, 47.

8 (*a*) S. Barata-Vallejo, S. M. Bonesi and A. Postigo, *Org. Biomol. Chem.*, 2015, **13**, 11153–11183; (*b*) T. Chatterjee, N. Iqbal, Y. You and E. J. Cho, *Acc. Chem. Res.*, 2016, **49**, 2284–2294; (*c*) S. Barata-Vallejo, M. V. Cooke and A. Postigo, *ACS Catal.*, 2018, **8**, 7287–7307; (*d*) S. Barata-Vallejo and A. Postigo, *Chem.–Eur. J.*, 2020, **26**, 11065–11084; (*e*) C. Czekelius, L. Helmecke, M. Spittler and B. M. Schmidt, *Synthesis*, 2020, **53**, 123–134.

9 (*a*) J. D. Nguyen, J. W. Tucker, M. D. Konieczynska and C. R. Stephenson, *J. Am. Chem. Soc.*, 2011, **133**, 4160–4163; (*b*) C. J. Wallentin, J. D. Nguyen, P. Finkbeiner and C. R. Stephenson, *J. Am. Chem. Soc.*, 2012, **134**, 8875–8884; (*c*) R. Beniazza, R. Atkinson, C. Absalon, F. Castet, S. A. Denisov, N. D. McClenaghan, D. Lastécouères and J.-M. Vincent, *Adv. Synth. Catal.*, 2016, **358**, 2949–2961; (*d*) E. Yoshioka, S. Kohtani, T. Jichu, T. Fukazawa, T. Nagai, A. Kawashima, Y. Takemoto and H. Miyabe, *J. Org. Chem.*, 2016, **81**, 7217–7229; (*e*) L.-L. Mao and H. Cong, *ChemSusChem*, 2017, **10**, 4461–4464; (*f*) Y. Wang, J. Wang, G. X. Li, G. He and G. Chen, *Org. Lett.*, 2017, **19**, 1442–1445; (*g*) T. Yajima and M. Ikegami, *Eur. J. Org. Chem.*, 2017, **15**, 2126–2129; (*h*) R. Beniazza, L. Remisse, D. Jardel, D. Lastecoueres and J. M. Vincent, *Chem. Commun.*, 2018, **54**, 7451–7454; (*i*) L. Helmecke, M. Spittler, K. Baumgarten and C. Czekelius, *Org. Lett.*, 2019, **21**, 7823–7827; (*j*) C. Rosso, G. Filippini, P. G. Cozzi, A. Gualandi and M. Prato, *ChemPhotoChem*, 2019, **3**, 193–197; (*k*) C. Rosso, G. Filippini and M. Prato, *Chem.–Eur. J.*, 2019, **25**, 16032–16036; (*l*) C. Rosso, J. D. Williams, G. Filippini, M. Prato and C. O. Kappe, *Org. Lett.*, 2019, **21**, 5341–5345; (*m*) E. Zhu, X. X. Liu, A. J. Wang, T. Mao, L. Zhao, X. Zhang and C. Y. He, *Chem. Commun.*, 2019, **55**, 12259–12262; (*n*) Y. X. Ji, L. J. Wang, W. S. Guo, Q. Bi and B. Zhang, *Adv. Synth. Catal.*, 2020, **362**, 1131–1137; (*o*) T. Mao, M. J. Ma, L. Zhao, D. P. Xue, Y. Yu, J. Gu and C. Y. He, *Chem. Commun.*, 2020, **56**, 1815–1818; (*p*) T. Yajima, M. Murase and Y. Ofuji, *Eur. J. Org. Chem.*, 2020, **2020**, 3808–3811.

10 (*a*) T. Rawner, E. Lutsker, C. A. Kaiser and O. Reiser, *ACS Catal.*, 2018, **8**, 3950–3956; (*b*) S. Engl and O. Reiser, *Eur. J. Org. Chem.*, 2020, **2020**, 1523–1533.

11 (*a*) J. Cao, G. Wang, L. Gao, H. Chen, X. Liu, X. Cheng and S. Li, *Chem. Sci.*, 2019, **10**, 2767–2772; (*b*) H. B. Yang, Z. H. Wang, J. M. Li and C. Wu, *Chem. Commun.*, 2020, **56**, 3801–3804.

12 (*a*) Q. Guo, M. Wang, Y. Wang, Z. Xu and R. Wang, *Chem. Commun.*, 2017, **53**, 12317–12320; (*b*) Q. Guo, M. Wang, Q. Peng, Y. Huo, Q. Liu, R. Wang and Z. Xu, *ACS Catal.*, 2019, **9**, 4470–4476; (*c*) M. Israr, H. Xiong, Y. Li and H. Bao, *Adv. Synth. Catal.*, 2020, **362**, 2211–2215.

13 N. J. Straathof, S. E. Cramer, V. Hessel and T. Noel, *Angew. Chem., Int. Ed.*, 2016, **55**, 15549–15553.

14 (*a*) D. Jing, C. Lu, Z. Chen, S. Jin, L. Xie, Z. Meng, Z. Su and K. Zheng, *Angew. Chem., Int. Ed.*, 2019, **58**, 14666–14672; (*b*) C. Lu, Z. Su, D. Jing, S. Jin, L. Xie, L. Li and K. Zheng, *Org. Lett.*, 2019, **21**, 1438–1443.

15 X.-C. Guo and Q.-Y. Chen, *J. Fluorine Chem.*, 1999, **93**, 81–86.

16 No conversion of **85** was observed at 80 °C in the dark for 8 h, indicating that **85** was stable at high temperature, and a radical pathway mediated by the thermal decomposition of **85** can be ruled out.

17 DFT calculation showed that the C–I bond dissociation energy (BDE) of **87** (56.0 kcal mol^{-1}) is higher than that of **85** (36.8 kcal mol^{-1}).

18 X. Sun, W. Wang, Y. Li, J. Ma and S. Yu, *Org. Lett.*, 2016, **18**, 4638–4641.